J. Phys. C: Solid St. Phys., 1971, Vol. 4. Printed in Great Britain

Diffraction in crystals at high energies

M. V. BERRY

H. H. Wills Physics Laboratory, Bristol

MS. received 30*th June* 1970, *in revised form* 12*th August* 1970

Abstract. By means of several distinct stages of approximation, the way in which wave propagation in a lattice becomes classical at high energies is analysed. First, the principle that deflection angles (whether caused by 'quantum' or 'classical' processes) are small at high energies is used to derive a simplified wave equation involving the lattice potential averaged along the direction of the incident beam. Next, the many-beam solution of this equation for the case of systematic reflections is presented in a form which emphasises the spatial variation of the potential, rather than its Fourier components. Third, approximate analytical expressions for the Bloch eigenvalues and eigenfunctions, and for the amplitudes of the diffracted beams, are derived by means of the WKB method; this leads to easily calculable expressions for the number of diffracted beams expected in a given situation, as well as for the number of Bloch waves contributing to these beams. Finally, the series of Bloch waves is transformed into a different series whose terms, suitably approximated, represent contributions to the diffraction amplitudes from topologically different classical paths.

1. Introduction

In recent years a controversy has developed in the field of high-energy particle propagation in lattices, concerning the distinction between situations where the full apparatus of quantum mechanics must be used to calculate observable quantities, and cases where it is sufficient to employ classical mechanics as an approximation (Chadderton 1968, Howie 1966, Cowley 1968). Both procedures have simple arguments to support them: for example, the smallness of the de Broglie wavelength λ in comparison with the interatomic distance a (even for 100 keV electrons in gold, $\lambda/a \sim 1/50$) suggests that the propagation is classical. On the other hand, the smallness of the deflection angles at high energies (a few degrees at most), suggests that a full many-wave treatment must be used since near-forward scattering is known to be dominated by quantum effects. For the reconciliation of these points of view it is necessary to have an analytical theory of the high-energy limit of quantum mechanics, and this is what the present paper attempts to provide. Only elastic scattering from a perfect crystal is considered, since inelastic and thermal effects complicate rather than dominate the picture. Even with this simplification, however, the analysis is complicated, and we proceed in four stages.

Firstly, in § 2, the general high-energy approximation to the relativistic Schrödinger equation is derived. This approximation has been used in the past (Howie 1966); it takes the form of a simplified Schrödinger-like equation involving only the projection of the lattice potential along the direction of the incident beam. The new derivation of the formalism that we give here is based on the near-forward nature of the scattering, and has the advantage of showing clearly the exact status of the phase grating approximation.

The general solution of the high-energy equation takes the form of a series of Bloch waves, whose number increases with increasing energy; the rest of the paper is devoted to an examination of this Bloch wave series for the case of systematic reflections, where only a single row of reciprocal lattice points contributes to the diffraction, and the projected potential varies in only one dimension. In § 3 the exact many-wave theory is developed in a form suitable for showing how the transition to the classical limit occurs.

The next step, in § 4, is to make use of the WKB method to derive approximate formulae for the Bloch wave eigenvalues and eigenfunctions.

Finally, in § 5, the eigenfunction series for the amplitudes of the diffracted beams is transformed with the aid of the Poisson summation formula into a series of integrals which are approximated by the method of stationary phase and shown to represent contributions from topologically different paths of particles that have travelled classically through the lattice and emerged in the directions of the various diffracted beams.

The mathematical techniques of §§ 4 and 5 are those commonly used in exploring the ways in which quantum phenomena approach their classical limits (Berry 1966, 1969 a), but the situation considered here has the additional complication that it is necessary to start by sorting out the 'high-energy' from the 'semiclassical' aspects of the problem.

2. High-energy formalism

We consider particles of rest mass m_0 and kinetic energy E incident on a crystal where the lattice potential is the real periodic function $V(\boldsymbol{r})$, $\boldsymbol{r}$ being a position vector. If spin effects are neglected (Fujiwara 1961, 1962), the wave function $\psi(\boldsymbol{r})$ is given by the solution of the Schrödinger equation

$$\{\nabla^2 + k^2 - U(\boldsymbol{r})\}\,\psi(\boldsymbol{r}) = 0 \tag{1}$$

where the wave number k and the reduced potential $U(\boldsymbol{r})$ are given by the relativistic expressions

$$\left.\begin{aligned} k &= \frac{1}{\hbar}(2m_0E + E^2/c^2)^{1/2} \\ U(\boldsymbol{r}) &= 2(m_0 + E/c^2)\,V(\boldsymbol{r})/\hbar^2 \end{aligned}\right\} \tag{2}$$

(note that the free-space wavelength λ is $2\pi/k$ and not $1/k$).

The incident beam is a plane wave with wave vector $\boldsymbol{k}_0$ (the length of $\boldsymbol{k}_0$ is of course k), and the crystal is a slab of thickness t whose faces have unit normal $\boldsymbol{n}$. For our first coordinate system we choose Cartesian axes such that $\boldsymbol{r} = (x, y, \zeta) = (\boldsymbol{R}, \zeta)$, where $\boldsymbol{R}$ is a two-dimensional vector describing position in planes $\perp O\zeta$. In this paper vectors denoted by capital letters will always be two dimensional; thus we write

$$\begin{aligned} \boldsymbol{k}_0 &= \{\boldsymbol{K}_0, (k^2 - K_0^2)^{1/2}\} \\ \boldsymbol{n} &= \{\boldsymbol{N}, (1 - N^2)^{1/2}\}. \end{aligned} \tag{3}$$

We shall later have to use a second coordinate system $\boldsymbol{r} = (\boldsymbol{R}, z)$ where Oz is parallel to $O\zeta$ but measured from zero at the entrance face of the crystal. Thus,

$$z = \zeta - \frac{\boldsymbol{R}\,.\,\boldsymbol{N}}{(1 - N^2)^{1/2}}. \tag{4}$$

These boundary conditions and coordinate systems are summarized in figure 1. Under typical diffraction conditions the angle between $\boldsymbol{k}_0$ and $\boldsymbol{n}$ is at most a few degrees, and the coordinate direction $O\zeta$ or Oz is chosen as the line most nearly parallel to $\boldsymbol{k}_0$ which is perpendicular to a low-index plane of reciprocal lattice points.

We can write the Schrödinger equation (1) in a form which incorporates the boundary condition involving the incident wave (Messiah 1962)

$$\psi(\boldsymbol{r}) = \exp(\mathrm{i}\boldsymbol{k}_0\,.\,\boldsymbol{r}) - \frac{1}{4\pi}\int \mathrm{d}\boldsymbol{r}'\,\frac{\exp(\mathrm{i}k|\boldsymbol{r} - \boldsymbol{r}'|)}{|\boldsymbol{r} - \boldsymbol{r}'|}\,U(\boldsymbol{r}')\,\psi(\boldsymbol{r}'). \tag{5}$$

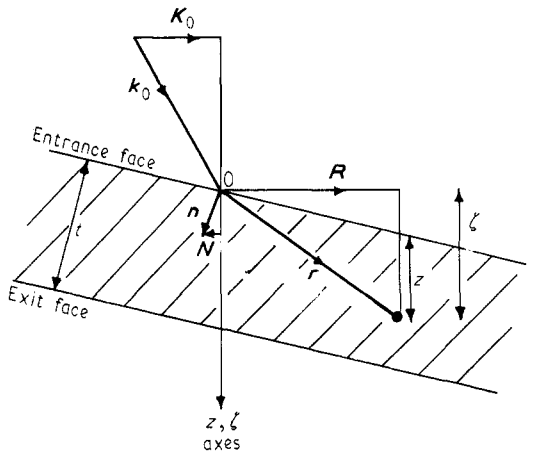

Figure 1. Geometry of incident wave, crystal slab and coordinate systems.

(It is of course necessary to set $U(\boldsymbol{r})$ equal to zero outside the slab.) If we define a reduced wave function $\rho(\boldsymbol{r})$ by

$$\psi(\boldsymbol{r}) = \exp(\mathrm{i}\boldsymbol{k}_0 \cdot \boldsymbol{r})\,\rho(\boldsymbol{r}) \tag{6}$$

and use the Fourier transform representation of the Green function in equation (5) we obtain

$$\rho(\boldsymbol{r}) = 1 + \frac{1}{(2\pi)^3}\int \mathrm{d}\boldsymbol{r}'\,\mathrm{d}\boldsymbol{q}'\,\frac{\exp\{\mathrm{i}(\boldsymbol{k}_0 - \boldsymbol{q})\cdot(\boldsymbol{r}' - \boldsymbol{r})\}}{k^2 - q^2 + \mathrm{i}\epsilon}\,\rho(\boldsymbol{r}')\,U(\boldsymbol{r}') \tag{7}$$

where ϵ is infinitesimal and positive.

It is simple to introduce the first coordinate system and use contour methods to integrate over q_ζ; this leads to the equation

$$\begin{aligned}\rho(\boldsymbol{r}) = 1 - \frac{\mathrm{i}}{8\pi^2}\int \mathrm{d}\boldsymbol{R}'\int \mathrm{d}\boldsymbol{Q}\,\frac{\exp\{\mathrm{i}(\boldsymbol{K}_0 - \boldsymbol{Q})\cdot(\boldsymbol{R}' - \boldsymbol{R})\}}{(k^2 - Q^2)^{1/2}} \\ \times\left(\int_{-\infty}^{\zeta} \mathrm{d}\zeta'\exp\left[\mathrm{i}\{(k^2 - K_0^2)^{1/2} - (k^2 - Q^2)^{1/2}\}(\zeta' - \zeta)\right]\right. \\ \left. + \int_{\zeta}^{\infty} \mathrm{d}\zeta'\exp\left[\mathrm{i}\{(k^2 - K_0^2)^{1/2} + (k^2 - Q^2)^{1/2}\}(\zeta' - \zeta)\right]\right)\rho(\boldsymbol{r}')\,U(\boldsymbol{r}')\end{aligned} \tag{8}$$

which is still exact.

In physical terms, equation (8) expresses the wave at a point $\boldsymbol{r}$ in terms of plane waves, whose wave-vectors have length k and all possible directions (specified by $\boldsymbol{Q}$), which have been scattered from all points $\boldsymbol{r}'$ in the slab. The secondary source points $\boldsymbol{r}'$ are divided into two groups, represented by the two integrals over ζ, which contribute waves to $\boldsymbol{r}$ by scattering into the forward and backward hemispheres. Now we know that no diffracted waves with appreciable magnitude emerge from the slab making angles of more than a few degrees with the direction $\boldsymbol{k}_0$ of the incident beam. Thus the only waves contributing significantly in equation (8) are those traveling almost parallel to $+\mathrm{O}\zeta$; the second 'back-scattered' integral can therefore be neglected, and in the first integral we can approximate the square roots in the exponent by

$$\left.\begin{aligned}(k^2 - Q^2)^{1/2} &\simeq k - \frac{Q^2}{2k} \\ (k^2 - K_0^2)^{1/2} &\simeq k - \frac{K_0^2}{2k}\end{aligned}\right\}. \tag{9}$$

The exponents in equation (8) also involve the depth coordinate ζ, and the condition for neglecting the remaining terms in the expansion of the square roots is

$$\frac{tQ^4}{8k^3} = \frac{kt\theta^4}{8} \ll 1 \tag{10}$$

where θ is a typical maximum diffraction angle.

For 4 MeV electrons in metallic foils 4000 Å thick this condition is violated if θ exceeds about two degrees. But the separation of neighbouring Bragg angles is about a minute of arc, so that the approximation (9) is valid, there being no diffracted beams whose order exceeds about a hundred. If the energy is only 100 keV, equation (10) is violated if θ exceeds about five degrees, and the approximation still holds with fair accuracy. Thus equation (9) is a suitable simplification to use over the whole range of high-energy diffraction conditions, and equation (8) becomes

$$\rho(\boldsymbol{r}) = 1 - \frac{\mathrm{i}}{8\pi^2 k}\int \mathrm{d}\boldsymbol{R}' \int \mathrm{d}\boldsymbol{Q} \exp\{\mathrm{i}(\boldsymbol{K}_0 - \boldsymbol{Q}).(\boldsymbol{R}' - \boldsymbol{R})\} \times \int_{-\infty}^{\zeta} \mathrm{d}\zeta' \exp\left\{\frac{\mathrm{i}(Q^2 - K_0^2)(\zeta' - \zeta)}{2k}\right\} \rho(\boldsymbol{r}')\, U(\boldsymbol{r}'). \tag{11}$$

The next step is to transfer to the second coordinate system, that is to introduce z and z' in place of ζ and ζ' with the aid of equation (4). The part of the exponent in equation (11) which involves $\boldsymbol{R} - \boldsymbol{R}'$ is changed to

$$(\boldsymbol{R}' - \boldsymbol{R}).\left\{\boldsymbol{K}_0 - \boldsymbol{Q} + \boldsymbol{N}\frac{Q^2 - K_0^2}{2k(1 - N^2)^{1/2}}\right\}.$$

The correction term involving $\boldsymbol{N}$ is of order θ^2 in comparison with the $\boldsymbol{K}_0 - \boldsymbol{Q}$ term, and may therefore be neglected; the lower limit of the z' integral is zero and equation (11) becomes

$$\rho(\boldsymbol{r}) = 1 - \frac{\mathrm{i}}{8\pi^2 k}\int \mathrm{d}\boldsymbol{R}' \int \mathrm{d}\boldsymbol{Q} \exp\{\mathrm{i}(\boldsymbol{K}_0 - \boldsymbol{Q}).(\boldsymbol{R}' - \boldsymbol{R})\} \times \int_{0}^{z} \mathrm{d}z' \exp\left\{\frac{\mathrm{i}(Q^2 - K_0^2)(z' - z)}{2k}\right\} \rho(\boldsymbol{r}')\, U(\boldsymbol{r}'). \tag{12}$$

Because of the quadratic dependence on the intermediate plane wave number $\boldsymbol{Q}$ in the exponent we may call this the *Fresnel approximation.*

To motivate the final stage of our derivation of the high-energy approximation, let us see what happens if we make an approximation more drastic than equation (9) to the square

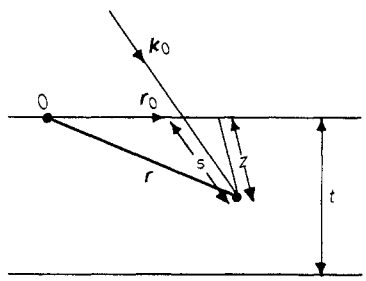

Figure 2. Ray coordinates used in the derivation of the phase grating approximation.

roots in equation (8). We expand to first order in the deviation $\boldsymbol{Q} - \boldsymbol{K}_0$ from the incident beam, that is, we write

$$Q^2 - K_0^2 = (\boldsymbol{Q} - \boldsymbol{K}_0).(\boldsymbol{Q} + \boldsymbol{K}_0) \simeq 2\boldsymbol{K}_0.(\boldsymbol{Q} - \boldsymbol{K}_0). \tag{13}$$

The condition for this to be valid is

$$\frac{(\boldsymbol{Q} - \boldsymbol{K}_0)^2 t}{2k} \sim \frac{kt\theta^2}{2} \ll 1 \tag{14}$$

which is far more restrictive than equation (10). The integral over $\boldsymbol{Q}$ in equation (12) is then simply a delta-function, and we obtain

$$\begin{aligned}\rho(\boldsymbol{r}) &= 1 - \frac{\mathrm{i}}{2k}\int \mathrm{d}\boldsymbol{R}' \int_0^z \mathrm{d}z'\, \delta\left(\boldsymbol{R}' - \boldsymbol{R} + \boldsymbol{K}_0 \frac{z - z'}{k}\right) \rho(\boldsymbol{r}')\, U(\boldsymbol{r}') \\ &= 1 - \frac{\mathrm{i}}{2k}\int_0^z \mathrm{d}z'\, \rho\left\{\boldsymbol{R} - \frac{\boldsymbol{K}_0(z - z')}{k}, z'\right\} U\left\{\boldsymbol{R} - \frac{\boldsymbol{K}_0(z - z')}{k}, z'\right\}.\end{aligned} \tag{15}$$

This equation means that only previous points along the incident ray through $\boldsymbol{r}$ contribute to the wave function at $\boldsymbol{r}$: to solve it, we introduce a coordinate system (figure 2) where s is the distance along the ray through $\boldsymbol{r}$ and $\boldsymbol{r}_0$ specifies the point where the ray enters the slab. To an accuracy of order θ^2, equation (15) becomes

$$\rho(\boldsymbol{r}_0, s) = 1 - \frac{\mathrm{i}}{2k}\int_0^s \mathrm{d}s'\, \rho(\boldsymbol{r}_0, s')\, U(\boldsymbol{r}_0, s') \tag{16}$$

which has the solution

$$\rho(\boldsymbol{r}) = \exp\left\{-\frac{\mathrm{i}}{2k}\int_0^s \mathrm{d}s'\, U(\boldsymbol{r}')\right\}. \tag{17}$$

This result is simply the well-known *phase grating approximation* (PGA) (Cowley and Moodie 1962); it involves the projection of the potential along the incident ray direction $\boldsymbol{k}_0$, and, in contrast to the Fresnel approximation (12), is only valid for very thin crystals.

If we do not make the PGA in equation (12) we can still integrate over $\boldsymbol{Q}$, and the result is

$$\begin{aligned}\rho(\boldsymbol{r}) = 1 - \frac{1}{4\pi}\int_0^z \mathrm{d}z' \frac{\exp\{-\mathrm{i}\, K_0^2(z' - z)/2k\}}{(z - z')} \\ \times \int \mathrm{d}\boldsymbol{R}' \left[\rho(\boldsymbol{r}')\, U(\boldsymbol{r}') \exp\{\mathrm{i}\boldsymbol{K}_0.(\boldsymbol{R}' - \boldsymbol{R}) + \frac{\mathrm{i}k(\boldsymbol{R} - \boldsymbol{R}')^2}{2(z - z')}\right].\end{aligned} \tag{18}$$

The quantity in brackets shows how the different parts $\boldsymbol{R}'$ of the layer at depth z' contribute to the wave at $\boldsymbol{R}$, z. The integral over $\boldsymbol{R}'$ converges because of the rapid oscillations of the Gaussian exponential factor where $|\boldsymbol{R} - \boldsymbol{R}'|$ is large. The contributing region at level z' is centred on the point $\boldsymbol{R}'_0$ where the phase is stationary

$$\boldsymbol{K}_0 + \frac{k(\boldsymbol{R} - \boldsymbol{R}'_0)}{z - z'} = 0$$

that is

$$\boldsymbol{R}'_0 = \boldsymbol{R} - \frac{\boldsymbol{K}_0(z - z')}{k} \tag{19}$$

(cf. equation (15)). A measure of the range of $\boldsymbol{R}'$ contributing to the integral is given by the radius $|\boldsymbol{R}' - \boldsymbol{R}'_0|$ at which the Gaussian exponent reaches the value π; this radius is

$$|\boldsymbol{R}' - \boldsymbol{R}'_0| = \{(2\pi/k)(z - z')\}^{1/2} = \{\lambda(z - z')\}^{1/2}. \tag{20}$$

The total region contributing to the wave field at $\boldsymbol{r}$ is thus a parabolic cone with apex at $\boldsymbol{r}$ and axis along the incident beam direction $\boldsymbol{k}_0$ (figure 3).

If t is small enough for the cones to be so thin at all points inside the slab that the potential $U(\boldsymbol{r}')$ does not vary significantly with $\boldsymbol{R}'$ within the cone at a level z', then the $\boldsymbol{R}'$ integral in equation (18) can be evaluated by the method of stationary phase, to yield once again the equation (15) that leads to the PGA. If the slab is thick then the upper parts of the cones

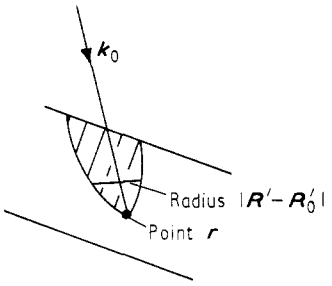

Figure 3. Region contributing to the wave field at $\boldsymbol{r}$.

will span several unit cells, and the PGA does not hold. But there is still a region of z' near to z for which the cone is thinner than, say, $a/10$, where a is a typical cell dimension; this region is easily calculated from equation (20) to be defined by

$$\frac{z-z'}{a} < \frac{a}{100\lambda} \tag{21}$$

a condition similar to equation (14) if we take θ to be about a Bragg angle. For electrons at 100 keV and 1 MeV, this means that $(z-z')$ must not exceed about one and five lattice spacings respectively. Thus the propagation proceeds according to the PGA over regions near the apex of the cone which are always larger than a lattice spacing, and, since the PGA involves the projection of the potential along $\boldsymbol{k}_0$ we do not need the full z-dependence of $U(\boldsymbol{r})$ in our equation (18), but only an average value, obtained by smearing $U(\boldsymbol{r})$ over a few lattice spacings in the direction $\boldsymbol{k}_0$.

To see how this smearing affects the periodic potential

$$U(\boldsymbol{r}) = \sum_{\boldsymbol{g}} U_{\boldsymbol{g}} \exp(\mathrm{i}\boldsymbol{g}\cdot\boldsymbol{r}) \tag{22}$$

(where the $\boldsymbol{g}$ are reciprocal lattice vectors) we average along $\boldsymbol{k}_0$ with a Gaussian weighting factor whose standard deviation (the 'smearing distance') is Δ; the resulting average potential is $\bar{U}(\boldsymbol{r})$ given by

$$\bar{U}(\boldsymbol{r}) = \sum_{\boldsymbol{g}} U_{\boldsymbol{g}} \exp(\mathrm{i}\boldsymbol{g}\cdot\boldsymbol{r}) \exp\{-(\boldsymbol{k}_0\cdot\boldsymbol{g})^2\,\Delta^2/2k^2\}. \tag{23}$$

This shows that only those lattice points contribute which lie on or near a plane $\perp \boldsymbol{k}_0$ (figure 4). If there is a low-index plane nearly $\perp \boldsymbol{k}_0$ (the *cross-grating* case) then we set our z-axis of coordinates $\perp$ to it; reciprocal lattice vectors are specified by $\boldsymbol{g} = (\boldsymbol{G}, g_z)$ and only the plane with $g_z = 0$ contributes to equation (23), since for the other planes

$$\frac{(\boldsymbol{k}_0\cdot\boldsymbol{g})^2}{2k^2}\Delta^2 > \frac{(2\pi)^2}{2a^2}\Delta^2 > 2\pi^2 \gg 1 \tag{24}$$

and the Gaussian exponential in (23) is utterly negligible. Since only the $g_z = 0$ plane contributes, the effective potential $\bar{U}(\boldsymbol{r})$ is periodic in $\boldsymbol{R}$ and independent of z. It is therefore periodic in the plane of the slab faces (which the original potential $U(\boldsymbol{r})$ is usually not), and this is the basic reason why diffraction can occur at all.

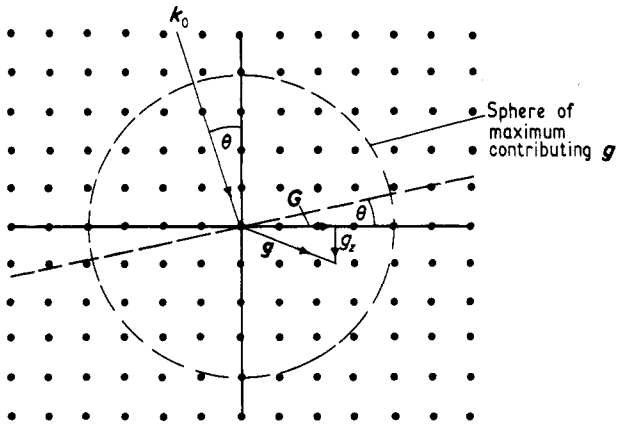

Figure 4. Geometry involved in averaging potential along k_0.

Now we examine the strength of contributions from those reciprocal lattice vectors which have $g_z = 0$. We assume that the angle θ between k_0 and Oz is about equal to the nth Bragg angle; for a G-point of order m, we obtain, using equation (21) to estimate Δ, that the Gaussian exponent in equation (23) is

$$(k_0 . g)^2 \frac{\Delta^2}{2k^2} \sim \frac{\theta^2}{2}\left(\frac{2\pi m}{a}\right)^2 \frac{a^4}{100^2\lambda^2} \sim \frac{1}{2}\left(\frac{n\lambda}{2a}\right)^2 \left(\frac{2\pi m}{a}\right)^2 \frac{a^4}{100^2\lambda^2} \sim \frac{m^2 n^2}{2000}$$

which is less than unity for most commonly-occurring m and n (m is limited by the fall-off of the U_g in the series (22)). The averaging therefore has the effect of simply eliminating from the series (22) all those U_g for which $g_z \neq 0$, and the resulting two-dimensionally periodic potential is

$$\bar{U}(\boldsymbol{R}) = \sum_{\boldsymbol{G}} U_{\boldsymbol{G}} \exp(\mathrm{i}\boldsymbol{G}.\boldsymbol{R}) \tag{25}$$

where the $U_{\boldsymbol{G}}$ are constants under normal diffraction conditions, given in terms of the assumed radially symmetric atomic reduced potential $\phi(r)$ by

$$U_{\boldsymbol{G}} = \frac{1}{\Omega}\int_{\text{cell}} \mathrm{d}\boldsymbol{R} \exp(\mathrm{i}\boldsymbol{G}.\boldsymbol{R}) \int_{-\infty}^{\infty} \mathrm{d}z\, \phi(R^2 + z^2)^{1/2} \tag{26}$$

where Ω is the volume of the real-space unit cell and the $\boldsymbol{R}$ integration is over the area of a face of the unit cell perpendicular to Oz.

If the reciprocal lattice plane most nearly perpendicular to k_0 is of low order only in the x direction, the y points will be too distant to contribute to equation (25), and the smeared potential will then vary only in the x direction. This is the case of *systematic reflections*. The periodic potential is then

$$\bar{U}(x) = \sum_n u(x - na) \tag{27}$$

where the one-dimensional layer potential is

$$u(x) = \frac{2\pi a}{\Omega}\int_{|x|}^{\infty} r\phi(r)\,\mathrm{d}r. \tag{28}$$

We are now in a position to finally derive the *general high-energy approximation* to the Schrödinger equation. Defining the new wave function $\tau(\boldsymbol{R}, z)$ by

$$\rho(\boldsymbol{r}) = \exp(-\mathrm{i}\boldsymbol{K}_0 . \boldsymbol{R})\,\tau(\boldsymbol{R}, z)$$

that is

$$\psi(\boldsymbol{r}) = \exp\{\mathrm{i}z(k^2 - K_0^2)^{1/2}\}\,\tau(\boldsymbol{R}, z) \tag{29}$$

substituting the smeared potential $\bar{U}(\boldsymbol{R})$ into equation (18), and differentiating, it is easy to show that τ satisfies the following wave equation, in which z behaves like a 'time' variable.

$$\left.\begin{aligned}\{\nabla_{\boldsymbol{R}}^2 + K_0^2 - \bar{U}(\boldsymbol{R})\}\,\tau(\boldsymbol{R}, z) &= -2\,\mathrm{i}k\frac{\partial\tau}{\partial z}(\boldsymbol{R}, z)\\ \tau(\boldsymbol{R}, 0) &= \exp(\mathrm{i}\boldsymbol{K}_0 . \boldsymbol{R})\end{aligned}\right\}. \tag{30}$$

There are other ways, perhaps less long-winded, of deriving what is essentially this approximation (Howie 1966), but the diffraction-theoretical methods used here bring out rather clearly the relationship with the PGA, and show how the averaging over the potential $U(\boldsymbol{r})$ arises in real space.

Since the potential is periodic, we can write τ as a Fourier series

$$\left.\begin{aligned}\tau(\boldsymbol{R}, z) &= \sum_{\boldsymbol{G}} A_{\boldsymbol{G}}(z)\exp\{\mathrm{i}(\boldsymbol{G} + \boldsymbol{K}_0).\boldsymbol{R}\}\\ A_{\boldsymbol{G}}(z) &= \frac{1}{S}\int_{\text{cell}} \mathrm{d}\boldsymbol{R}\,\tau(\boldsymbol{R}, z)\exp\{-\mathrm{i}(\boldsymbol{G} + \boldsymbol{K}_0).\boldsymbol{R}\}\end{aligned}\right\} \tag{31}$$

where $A_{\boldsymbol{G}}(z)$ is the amplitude of the $\boldsymbol{G}$th diffracted beam at level z and S is the area of a cell face in the $\boldsymbol{R}$ plane. At the exit face $z = t$ these diffracted beams will be transmitted out of the slab (there will be a very small amount of reflection and refraction which we neglect—it can easily be taken into account) and propagate undisturbed in free space with wave vectors $[\boldsymbol{K}_0 + \boldsymbol{G}, \{k^2 - (\boldsymbol{K}_0 + \boldsymbol{G})^2\}^{1/2}]$; it is these diffracted beams that are observed, and the $A_{\boldsymbol{G}}(z)$ are the functions that any theory must predict. Substitution of equation (31) into equation (30) gives, for the amplitudes:

$$\left.\begin{aligned}\frac{\partial A_{\boldsymbol{G}}(z)}{\partial z} &= -\frac{\mathrm{i}}{2k}\sum_{\boldsymbol{G}'} A_{\boldsymbol{G}'}(z)\,U_{\boldsymbol{G}-\boldsymbol{G}'} - \frac{\mathrm{i}}{2k}(G^2 + 2\,\boldsymbol{G}.\boldsymbol{K}_0)\,A_{\boldsymbol{G}}(z)\\ A_{\boldsymbol{G}}(0) &= \delta_{\boldsymbol{G},0}\end{aligned}\right\} \tag{32}$$

a differential–difference equation that has appeared in the literature in various guises during the past 35 years (Raman and Nath 1936, Gill 1964, Howie and Whelan 1961). It is easy to show from this equation that for a real lattice potential the sum rule

$$\sum_{\boldsymbol{G}} |A_{\boldsymbol{G}}(z)|^2 = 1 \tag{33}$$

holds for all z.

The analytic behaviour of solutions to differential–difference equations is not well understood, so we shall not use equation (32) to explore the classical limit. It can be shown, however, that the PGA results from setting the term involving G^2 equal to zero in equation (32) (this statement can be made plausible by putting $\boldsymbol{Q} = \boldsymbol{K}_0 + \boldsymbol{G}$ in equation (13)), and this result is sufficient to show that the PGA will never predict the phenomenon of specular Bragg reflection from the potential $\bar{U}(\boldsymbol{R})$. The reason, briefly, is that the enhancement of the $\boldsymbol{G}_1$ reflection that we call specular Bragg reflection occurs for small $U_{\boldsymbol{G}}$ when the incident direction $\boldsymbol{K}_0$ is chosen such that the term $G_1^2 + 2\boldsymbol{K}_0 . \boldsymbol{G}_1$ is zero in equation (32), that is, when

$$\boldsymbol{K}_0 = -\boldsymbol{G}_1/2 \tag{34}$$

which is just the condition for specular Bragg reflection; when the PGA is made, the connection between equations (34) and (32) is lost. Work is in progress examining the value of analogue computation for solving equation (32); this technique has already proved valuable

in solving the simpler but similar problem of the diffraction of light by ultrasound (Berry 1967).

To get a form of many-wave theory suitable for showing the transition to the classical limit we decompose the wave function $\tau(\boldsymbol{R}, z)$ into eigenfunctions by separating out the z coordinate, that is we write

$$\tau(\boldsymbol{R}, z) = [\sum_j C_j \tau_j(\boldsymbol{R}) \exp(-\mathrm{i}s_j z/2k)] \exp(\mathrm{i}K_0^2 z/2k) \tag{35}$$

where the $\tau_j(\boldsymbol{R})$ are those solutions (normalized over a cell face in the $\boldsymbol{R}$ plane) of

$$\{\nabla_{\boldsymbol{R}}^2 + s_j - \bar{U}(\boldsymbol{R})\}\, \tau_j(\boldsymbol{R}) = 0 \tag{36}$$

which are continuous in slope and value and periodic but for a modulating factor $\exp(\mathrm{i}\boldsymbol{K}_0 . \boldsymbol{R})$. The completeness relation for eigenfunctions can be used to show that the weighting factors C_j which are needed to make $\tau(\boldsymbol{R}, z)$ satisfy the boundary condition in equation (30) at $z = 0$ are given by

$$C_j = \int_{\text{cell}} \mathrm{d}\boldsymbol{R}\, \tau_j^*(\boldsymbol{R}) \exp(\mathrm{i}\boldsymbol{K}_0 . \boldsymbol{R}). \tag{37}$$

We have arrived, then, at a two-dimensional Bloch-wave problem where the Bloch wave vector $\boldsymbol{K}_0$ is given and the 'energy' s_j is to be found. The diffraction amplitudes are given by

$$A_{\boldsymbol{G}}(z) = \frac{\exp(\mathrm{i}K_0^2 z/2k)}{S} \sum_j \left\{ \int_{\text{cell}} \mathrm{d}\boldsymbol{R}\, \tau_j^*(\boldsymbol{R}) \exp(\mathrm{i}\boldsymbol{K}_0 . \boldsymbol{R}) \right\}$$
$$\times \left[\int_{\text{cell}} \mathrm{d}\boldsymbol{R}\, \tau_j(\boldsymbol{R}) \exp\{-\mathrm{i}(\boldsymbol{K}_0 + \boldsymbol{G}) . \boldsymbol{R}\} \right] \exp(-\mathrm{i}s_j z/2k). \tag{38}$$

To see the effect of increasing the energy E in our equations it is sensible at the same time to decrease the angle of incidence so that $\boldsymbol{K}_0$ remains constant (for instance we may be illuminating the crystal at exact Bragg incidence for the $\boldsymbol{G}_1$ reflection, in which case $\boldsymbol{K}_0$ is given by equation (34) which is independent of E). Then the only way that τ_j, s_j and C_j can change (equations (36) and (37)) is through the relativistic energy dependence of the potential $\bar{U}(\boldsymbol{R})$ (see equation (2)). This is what alters the number of Bloch waves, that is the number of non-negligible C_j in the calculation; we shall see that the limit where there are many waves is the classical limit, so that the increasing 'classicality' at high energies is entirely a relativistic effect. In the case of electrons there are only a few contributing Bloch waves up to about 1 MeV, above which the classical description should gradually become more applicable; for protons, however, their large mass means that the $U_{\boldsymbol{G}}$ are large enough for a classical description to be appropriate for any energy above about 100 keV. As well as the number of beams increasing with E, the variation of the exponential contributions to the z dependence of $A_{\boldsymbol{G}}$ slows down due to the nonrelativistic decrease of the exponent $s_j z/2k$. For an alternative approach to the high-energy approximation, see Lervig *et al.* (1967).

3. Exact many-wave theory for case of systematic reflections

For electrons scattered from an atom of charge Z, the atomic potential takes the form

$$\phi(r) = -\frac{Ze^2}{4\pi\epsilon_0 r} \chi(r) \tag{39}$$

where $\chi(r)$ is a screening function that drops from the constant value unity near $r = 0$, to zero when r is about an atomic radius. In the corresponding one-dimensional layer potential $u(x)$, given by equation (28), the Coulomb singularity is modified to a discontinuity of slope at the atomic planes; the smooth distribution of charge between the atoms means

that there is a parabolic potential barrier between the atomic planes, so that the whole periodic potential in the case of systematic reflections has the form shown in figure 5(*a*), where the zero of x is taken *between* atomic planes, and the zeroth cell runs from $x = -a/2$ to $x = +a/2$. In the case of positively-charged particles the potential is reversed in sign, but we again take $x = 0$, the centre of the zeroth cell, as the point of maximum potential,

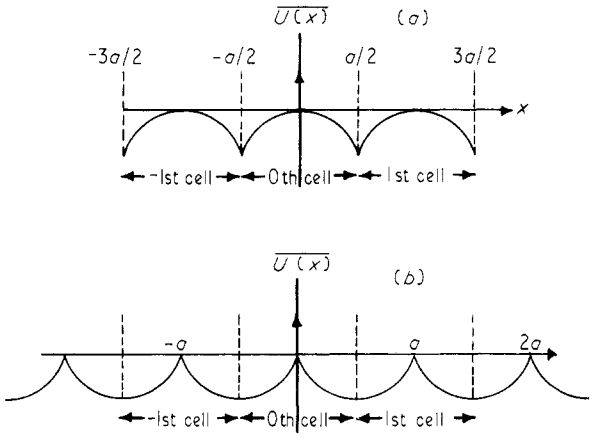

Figure 5. One-dimensional potential for: (*a*) negative particles, atomic planes at ..., $-a/2$, $a/2$, $3a/2$ etc. (*b*) positive particles, atomic planes at ..., $-a$, 0, a, $2a$, $3a$ etc.

which now lies *on* an atomic plane (figure 5(*b*)); the point is that $u(x)$ always has the form of a potential barrier, whose top is parabolic for negative particles and cusped for positive particles (for the simpler problem of the diffraction of light by ultrasound, $\overline{U}(x)$ is sinusoidal).

Let $\tau_1(x, s)$ be any solution in the zeroth cell $|x| < a/2$ of

$$\left\{\frac{d^2}{dx^2} + s - U(x)\right\}\tau(x, s) = 0 \tag{40}$$

which is the one-dimensional version of equation (36). Then, since the potential $u(x)$ is even an independent solution is given by

$$\tau_2(x, s) = \tau_1(-x, s) \tag{41}$$

so that the eigenfunctions are a linear combination of τ_1 and τ_2 namely

$$\tau_j(x) = A_j\tau_1(x, s_j) + B_j\tau_2(x, s_j) \tag{42}$$

where the eigenvalues s_j and the coefficients A_j and B_j are to be determined by the boundary conditions. In the first cell $a/2 \leqslant x \leqslant 3a/2$, τ_j is given by

$$\tau_j(x + a) = \exp(iK_0a)\,\tau_j(x) = \exp(iK_0a)\,(A_j\tau_1(x, s_j) + B_j\tau_2(x, s_j))$$

which must be continuous in slope and value at the cell boundary $x = a/2$ with the solution (42), so that

$$\left.\begin{aligned} A_j\tau_1(a/2, s_j) + B_j\tau_2(a/2, s_j) &= \exp(iK_0a)\,\{A_j\tau_1(-a/2, s_j) + B_j\tau_2(-a/2, s_j)\} \\ A_j\tau_1'(a/2, s_j) + B_j\tau_2'(a/2, s_j) &= \exp(iK_0a)\,\{A_j\tau_1'(-a/2, s_j) + B_j\tau_2'(-a/2, s_j)\} \end{aligned}\right\} \tag{43}$$

where the primes denote differentiation with respect to x.

In order to interpret these boundary conditions, we take for our basic solution $\tau_1(x, s)$ the wave function that results when a plane wave is incident from the left on the potential barrier in the zeroth cell. There will be a reflected wave of amplitude $R(s)$ for $x < -a/2$

and a transmitted wave of amplitude $T(s)$ for $x > a/2$. The wave number of the waves outside the cell is

$$\gamma = \{s - \bar{U}(-a/2)\}^{1/2} \tag{44}$$

which is always real and positive. Schematic representations of the basic solutions τ_1 and τ_2 are shown in figure 6. Use of these wave functions in equation (43) gives, after a little algebra,

$$\frac{A_j}{B_j} = \frac{\exp(-i\gamma a) - T\exp(iK_0 a)}{R\exp(iK_0 a)} = \frac{R\exp(i\gamma a)}{\exp(iK_0 a) - T\exp(i\gamma a)} \tag{45}$$

To simplify these conditions we use the relations

$$\left.\begin{aligned} |R|^2 + |T|^2 &= 1 \\ R^*T + RT^* &= 0 \end{aligned}\right\} \tag{46}$$

where the first is a consequence of the conservation of current for the wave function $\tau_1(x)$ and the second is derived by comparing the 'reversed' function $\tau_2(x)$ as given by figure 6

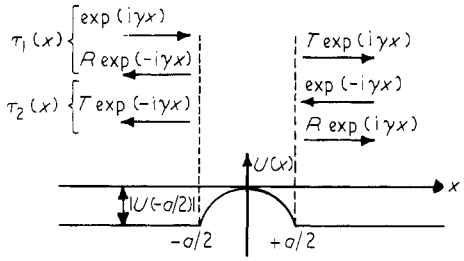

Figure 6. Independent barrier wave functions.

with an alternative form made up of a linear combination of $\tau_1(x)$ and $\tau_1^*(x)$. If the phase of T is μ, so that

$$T = |T|\exp(i\mu) \tag{47}$$

then, from equation (46), we have

$$R = -i\exp(i\mu)|(1 - |T|^2)^{1/2}| \tag{48}$$

where the negative sign comes from inspection of the behaviour of known solutions of Schrödinger's equation.

If we combine the second member of equation (45) with equations (46)–(48) we obtain after some reduction an equation for the eigenvalues s_j

$$|T|\cos K_0 a = \cos(\gamma a + \mu) \tag{49}$$

where $|T|$, γ and μ depend on s_j (see also Taylor 1970, Howie 1967). The first member of equation (45), together with equations (46)–(49) gives, for the relative contributions of the two solutions τ_1 and τ_2

$$\frac{A_j}{B_j} = \exp(-iK_0 a)\frac{\sin(\gamma a + \mu + K_0 a)|\cos K_0 a|}{|\{\cos^2 K_0 a - \cos^2(\gamma a + \mu)\}^{1/2}|\cos K_0 a} \tag{50}$$

The final condition which enables A_j, B_j and s_j to be determined is the normalization relation, which becomes, if equation (42) is used,

$$\int_{-a/2}^{a/2} |\tau_j(x)|^2 \, dx = (|A|^2 + |B|^2) \int_{-a/2}^{a/2} |\tau_1|^2 \, dx + 2\mathrm{Re}\{A^*B \int_{-a/2}^{a/2} \tau_1^*(x)\tau_2(x) \, dx\} = 1. \quad (51)$$

To get a feeling for the basic relations (49) and (50), it is helpful to look at some special cases. First, we take the case of illumination at the nth Bragg angle, where

$$K_0 = K_0^{(n)} = -\frac{G_n}{2} = -\frac{n\pi}{a}. \quad (52)$$

Then equation (50) is

$$\frac{A_j}{B_j} = (-1)^n \frac{\sin(\gamma a + \mu)}{|\sin(\gamma a + \mu)|} = (-1)^{n+j} \quad (53)$$

since a simple graphical exploration of the solutions of equation (49) (see § 4 and figure 9) soon reveals that $\sin(\gamma a + \mu)$ alternates in sign for successive values of s_j. Equation (53) shows that at the Bragg angles the eigenfunctions are either purely even or purely odd, on account of equation (41).

The second special case we shall consider is when the transmission coefficient $|T|$ is zero. This condition is approximated when there are solutions of equation (49) for which s_j is large and negative, because the wave hardly tunnels at all through the high potential barrier. Then equation (49) shows that the eigenvalues are independent of K_0, being given by

$$\gamma(s_j)\, a + \mu(s_j) = (j + \tfrac{1}{2})\, \pi \quad (54)$$

so that equation (50) becomes

$$\frac{A_j}{B_j} = (-1)^j \exp(-iK_0 a). \quad (55)$$

For this special case the wave-functions τ_1 and τ_2 can be chosen to be real, and the eigenfunctions are represented schematically in figure 7; this is the 'tight-binding' situation, where the 'energy bands' are narrow, and centred on the values of s_j given by equation (54).

The last case we shall consider is the 'nearly-free' case, which occurs for large positive s_j,

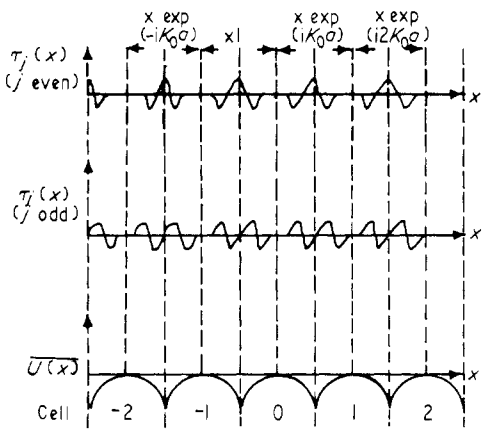

Figure 7. Schematic representation of 'tight-binding' eigenfunctions. where $|T| = 0$.

where the particles hardly see the barrier and the reflection coefficient $|R|$ is zero, $|T|$ being unity. Then (49) gives

$$\gamma(s_j^{\pm})\, a + \mu(s_j^{\pm}) = \pm K_0 a + 2j\pi \tag{56}$$

and equation (50) becomes indeterminate, so that we have to return to equation (45); a little inspection then shows that

$$\begin{aligned} B &= 0 \qquad \text{if} \quad s_j = s_j^{+} \\ A &= 0 \qquad \text{if} \quad s_j = s_j^{-} \end{aligned} \tag{57}$$

and the eigenfunctions are simply travelling waves passing without attenuation through the lattice, while the band gaps are narrow since all values of s_j are predicted by equation (56).

4. WKB approximations to many-wave theory

When the potential $\overline{U}(x)$ is large, (what we mean by large will become clear later), the two special cases where $|T|$ is nearly zero and nearly unity are separated by only a narrow range of values of s, near to zero (the top of the barrier). If $x_0^{\pm}(s)$ are the two classical turning points which exist for negative s, namely the solutions of

$$[s - \overline{U}\{x_0(s)\}]^{1/2} = 0 \tag{58}$$

then the semiclassical expression for the modulus of the transmission coefficient $|T|$ in the case where the incident particles are negatively charged (figure 5(*a*)) is (Miller and Good 1953)

$$|T(s)| = \left(1 + \exp\left[2\int_{x_0^-}^{x_0^+} \{\overline{U}(x) - s\}^{1/2}\, \mathrm{d}x\right]\right)^{-1/2} \tag{59}$$

This expression is valid through the barrier top region and when $s > 0$ (where $x_0^{\pm}$ are the complex solutions of equation (58)). Since the integral in equation (59) changes from positive to negative as s changes from negative to positive, $|T|$ varies from exponentially small below the barrier to a quantity that differs only to an exponentially small degree from unity above the barrier.

It is possible to obtain a semiclassical approximation for the 'barrier' wave function $\tau_1(x, s)$ which is valid (for large potentials) uniformly for all values of x and s (Miller and Good 1953): this involves parabolic cylinder functions, and is the best analytical approximation to use for numerical calculations of the Bloch wave amplitudes. However, for exploring the classical limit such a sophisticated approach is not necessary, and we can use separate approximations for the free ($|T| = 1$) and bound ($|T| = 0$) regions, since we shall see that the region near $s = 0$, where both approximations breakdown, diminishes in importance as we approach classical conditions. The WKB approximations involve the classical phase integral $\phi(a, b; s)$ (we shall occasionally suppress the s dependence) defined by

$$\phi(a, b; s) = \int_a^b \{s - \overline{U}(x)\}^{1/2}\, \mathrm{d}x. \tag{60}$$

The above-barrier solution is then (Heading 1962, p. 26) the travelling wave

$$\tau_1(x, s) = \frac{\exp\{\mathrm{i}\phi(0, x)\}}{\{s - \overline{U}(x)\}^{1/4}}. \tag{61}$$

Below the barrier top, the form of solution which is valid through the turning point $x_0^-(s)$ into the classically forbidden region is

$$\tau_1(x, s) = \frac{\{\frac{3}{2}\phi(x, x_0^-)\}^{1/6}}{\{s - \overline{U}(x)\}^{1/4}}\, \mathrm{Ai}\,[-\{\tfrac{3}{2}\phi(x, x_0^-)\}^{2/3}] \tag{62}$$

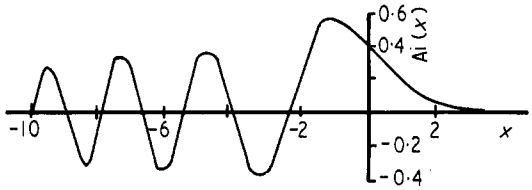

Figure 8. The Airy function.

where Ai(x) (figure 8) is the Airy function (Dingle 1956) (see also figure 7). For $x < x_0^-$, in the classically allowed region, we can use the asymptotic form of the Airy function to give

$$\tau_1(x, s) = \frac{\sin\{\phi(x, x_0^-) + \pi/4\}}{\sqrt{\pi}\{s - \bar{U}(x)\}^{1/4}} \qquad (x < x_0^-(s)). \tag{63}$$

By inspection of equations (61) and (63) and comparison with equation (47) it is possible to see that for all s

$$\gamma a + \mu = 2\phi(-a/2, x_0^-) \tag{64}$$

$$= \mathrm{Re}\int_{-a/2}^{a/2} \mathrm{d}x\,\{s - \bar{U}(x)\}^{1/2} \equiv \Phi(s) \tag{65}$$

where only the classically allowed region in a unit cell contributes to the integral. Thus we can solve the basic condition (49) for the eigenvalues s_j by using equations (59) and (65) and plotting $|T(s)|\cos K_0 a$ and $\cos\Phi(s)$ against s and finding the intersections of the two curves (figure 9).

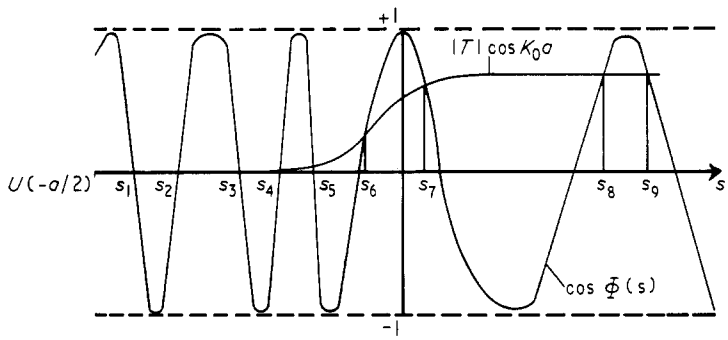

Figure 9. Graphical solution of equation for eigenvalues s_j.

In the case where the incident particles are positively charged, and the barrier top has a discontinuity of slope (figure 5*b*) the solutions for $|T| \backsim 0$ or 1 are still given by equations (62) and (61) but as s increases from zero $|T|$ varies not like equation (59) but according to

$$|T| \simeq 1 - \frac{\{(\mathrm{d}\bar{U}/\mathrm{d}x)(x = \quad)\}^2}{8\,s^3} \qquad (s \gg 0) \tag{66}$$

which approaches unity rapidly enough for figure 9 to be qualitatively correct for this case also.

Now let us use the solutions (61) and (63) to construct the normalized eigenfunctions τ_j. Above the barrier top ($s > 0$) the τ_j are alternately forward- and backward-travelling waves (see equations (56) and (57)) and, using an obvious notation,

$$\tau_j^{\pm}(x) = \frac{\exp\{\pm\,\mathrm{i}\phi(0, x; s_j^{\pm})\}}{\{s_j^{\pm} - \bar{U}(x)\}^{1/4}\,[2\int_{-a/2}^{0} \mathrm{d}x/\{s_j^{\pm} - \bar{U}(x)\}^{1/2}]^{1/2}} \tag{67}$$

Below the barrier top ($s < 0$) it is not hard to show that the normalization integral is insensitive under semiclassical conditions to whether we choose equation (62) (where the wave function has an exponentially-decaying tail in the classically forbidden barrier region) or equation (63) (where we take the wave function as zero for $x > x_0^-(s)$). There is no overlap between τ_1 and τ_2, so that the second integral in equation (51) is zero, and $|A/B|$ is unity, from equation (55), so that, below the barrier top,

$$\tau_j(x) = \frac{\sin\{\phi(x, x_0^-; s_j) + \pi/4\}}{\{s_j - \bar{U}(x)\}^{1/4}\,[2\int_{-a/2}^{x_0^-(s_j)} \mathrm{d}x \sin^2\{\phi(x, x_0^-; s_j) + \pi/4\}/\{s_j - \bar{U}(x)\}^{1/2}]^{1/2}}. \tag{68}$$

But the integrand in the denominator can be approximated by setting $\sin^2$ equal to $\frac{1}{2}$, because the error thus incurred is to neglect an oscillatory integral, a procedure justified under semiclassical conditions. Thus

$$\left.\begin{aligned} \tau_j(x) &= \frac{\sin\{\phi(x, x_0^-; s_j) + \pi/4\}}{\{s_j - \bar{U}(x)\}^{1/4}\,[\int_{-a/2}^{x_0^-(s_j)} \mathrm{d}x/\{s_j - \bar{U}(x)\}^{1/2}]^{1/2}} && (x < x_0^-) \\ &= 0 && |x| < |x_0| \\ &= \frac{(-1)^j \exp(\mathrm{i}K_0 a)\sin\{\phi(x_0^+, x; s_j) + \pi/4\}}{\{s_j - \bar{U}(x)\}^{1/4}\,[\int_{-a/2}^{x_0^-(s_j)} \mathrm{d}x/\{s_j - \bar{U}(x)\}^{1/2}]^{1/2}} && (x > x_0^+) \end{aligned}\right\} \tag{69}$$

(we have made use of equation (55)).

Once again we assert that the fact that these wave functions diverge at the classical turning-points $x_0^{\pm}(s_j)$ will not affect the passage to the classical limit.

Now we have to insert the solutions (67) and (69) into the many-wave expression (38) for the amplitudes of the diffracted beams; if we write

$$\boldsymbol{K}_G \equiv \boldsymbol{K}_0 + \boldsymbol{G} \tag{70}$$

then the one-dimensional form of equation (38) appropriate for the case of systematic reflections, is

$$\begin{aligned} A_G(z) = {} & \frac{\exp(\mathrm{i}K_0^2 z/2k)}{a} \sum_j \left\{ \int_{-a/2}^{a/2} \mathrm{d}x\, \tau_j^*(x) \exp(\mathrm{i}K_0 x) \right\} \\ & \times \left\{ \int_{-a/2}^{a/2} \mathrm{d}x\, \tau_j(x) \exp(-\mathrm{i}K_G x) \right\} \exp(\mathrm{i}s_j z/2k). \end{aligned} \tag{71}$$

The integrands in this expression are combinations of oscillatory exponential functions, and the largest contributions come from those values of j where both exponents have stationary points somewhere in the zeroth unit cell. For values of j where there are no stationary points the main contributions come from the end points, but under semiclassical conditions these are smaller than the stationary-point contributions by a factor of order

$$\{|u(-a/2)|a\}^{-1/2}$$

(for a good account of these asymptotic methods, see Erdelyi 1956, Chap. II). The condition for a stationary point in the integral involving s is obtained by differentiating the exponent; making use of equation (60), the result is

$$\{s - \bar{U}(x)\}^{1/2} = |K| \tag{72}$$

where K represents K_0 or K_G. The solutions of this equation, if there are any, are

$$x \equiv x_K^{\pm}(s) \tag{73}$$

a notation consistent with equation (58) when K is zero.

A simple graphical construction (figure 10) shows that the Bloch waves contributing to each of the integrals in equation (71) are those where the eigenvalues s_j lie within a band of width $|u(-a/2)|$ whose upper edge is at

$$s_j^{\max} = K^2. \tag{74}$$

The x wave number is K_0 for the first integral in equation (71) and K_G for the second so that the Bloch waves contributing significantly to $A_G(z)$ will be those lying in the region where the two bands overlap. For the 'reflected' beams, where the signs of K for the incident and diffracted beams K_0 and K_G are different, there is no contribution to A_G from the 'free'

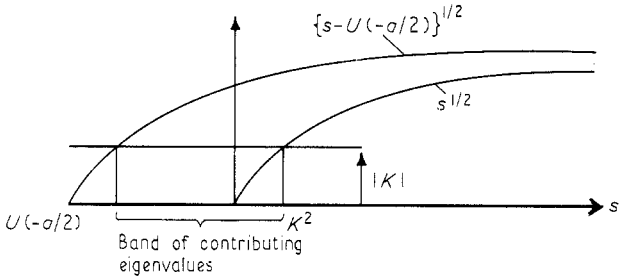

Figure 10. Significant Bloch waves contributing to integrals for amplitudes of diffracted beams.

states (with $s > 0$), since (cf. equations (57) and (67)) if K is positive only the + eigenstate integrands have stationary points, and *vice versa*. An analysis of the overlap which takes account of this property of the 'reflected' beams leads to results which differ according to whether $|K_0|$ is greater or less than the critical value

$$|K_0^c| = \{|u(-a/2)|\}^{1/2} \tag{75}$$

corresponding to a critical angle of incidence

$$\theta_c = \{|u(-a/2)|\}^{1/2}/k. \tag{76}$$

It is helpful to imagine K_0 as positive; this involves no loss of generality. Then if $K_G^{\pm}$ are the wave numbers of the diffracted beams which suffer the greatest $\pm$ deviation from K_0, we have:

$$\left.\begin{aligned} K_G^+ &= +\{K_0^2 + |u(-a/2)|\}^{1/2} \\ K_G^- &= -\{|u(-a/2)|\}^{1/2} \end{aligned}\right\} \theta < \theta_c$$
$$\left.\begin{aligned} K_G^+ &= +\{K_0^2 + |u(-a/2)|\}^{1/2} \\ K_G^- &= +\{K_0^2 - |u(-a/2)|\}^{1/2} \end{aligned}\right\} \theta > \theta_c \tag{77}$$

(see figure 11).

Thus when $\theta > \theta_c$ there are no 'reflected' waves, and *a fortiori* no vestige of Bragg reflection, which is an enhancement of the 'reflected' beam for which K_G equals $-K_0$. If the nth reciprocal lattice point is defined as in equation (52), then the highest positive and negative orders of diffraction $n\pm$ are given by

$$\left.\begin{aligned} n^+ &= \frac{a}{2\pi}[\{K_0^2 + |u(-a/2)\}^{1/2} - K_0] \\ n^- &= -\frac{a}{2\pi}[\{|u(-a/2)|\}^{1/2} + K_0] \end{aligned}\right\} \quad \theta < \theta_c \tag{78}$$

$$\left.\begin{aligned} n^+ &= \frac{a}{2\pi}\left[\{K_0^2 + |u(-a/2)|\}^{1/2} - K_0\right] \\ n^- &= -\frac{a}{2\pi}\left[K_0 - \{K_0^2 - |u(-a/2)|\}^{1/2}\right] \end{aligned}\right\} \theta > \theta_c \tag{78}$$

so that for normal incidence, for example, the total number of significant diffracted beams is

$$\mathcal{N} = 2n^+ + 1 = \frac{a}{\pi}\{|u(-a/2)|\}^{1/2} + 1. \tag{79}$$

This expression also gives the number of Bragg resonances passed through by the direction of incidence as it varies from $\theta = 0$ to $\theta = \theta_c$.

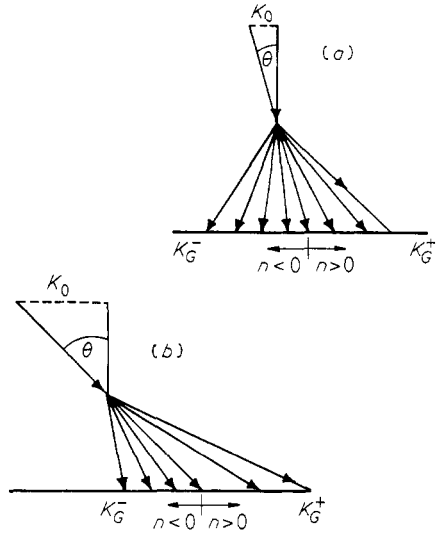

Figure 11. Diffracted beams when: (*a*) $\theta < \theta_c$; (*b*) $\theta > \theta_c$.

With the equations (77) we make direct contact for the first time with the classical mechanics of the propagation problem. The simplest way to see this is to notice that equation (40) represents a problem where the 'transverse energy' is given in Hamiltonian form by

$$s = K^2 + \bar{U}(x) \tag{80}$$

since K, the transverse wave number, is the momentum conjugate to the coordinate x. From equation (30), the quantity corresponding to time is the depth coordinate z. Thus a given ray, specified by a point of entry $x(0)$ to the slab at $z = 0$ and an initial momentum K_0, propagates so that at any subsequent depth its position $x(z)$ and momentum $K(z)$ are such that

$$s = K_0^2 + u\{x(0)\} = K(z)^2 + \bar{U}\{x(z)\} = \text{constant}. \tag{81}$$

Thus for a given K_0, as $x(0)$ varies from $-a/2$ to 0, s takes on values spanning the band given by equation (74) and figure 10. The only possible values of the exit momentum $K(z)$ are given by

$$K(z) = [K_0^2 + u(x_0) - \bar{U}\{x(z)\}]^{1/2} \tag{82}$$

as x_0 and $x(z)$ vary within the cell. If we take account of the fact that $K(z)$ and K_0 can only differ in sign if K passes smoothly through zero at some intermediate depth, then inspection of the classical equation (82) yields precisely the same conditions as equation (77) which were derived by applying the WKB method to the quantum-mechanical many wave formalism. The importance of the critical angle θ_c is well established in classical channeling theory (Lindhart 1965).

As well as calculating the number of diffracted beams that are likely to appear for a given energy E and direction of incidence K_0, we now have enough information to find out the number $N(K_0)$ of Bloch waves j which contribute in the many-wave expression (71) for $A_G(z)$. From equations (65), (54) and (56), it is easy to show that the maximum number $N_0(K_0)$, which occurs for the zeroth-order undeviated beam where K_G equals K_0, is

$$\left.\begin{aligned} N_0(K_0) &= \frac{\Phi(K_0^2) + \Phi(0) - 2\Phi\{K_0^2 - |u(-a/2)|\}}{2\pi} && \theta < \theta_c \\ &= \frac{\Phi(K_0^2) - \Phi\{K_0^2 - |u(-a/2)|\}}{2\pi} && \theta > \theta_c \end{aligned}\right\} \tag{83}$$

For normal incidence this reduces to the simple expression

$$N_0(0) = \frac{\Phi(0)}{\pi} = \frac{\int_{-a/2}^{a/2} \{-u(x)\}^{1/2}\,\mathrm{d}x}{\pi} \tag{84}$$

but for this case the odd bound solutions do not contribute (see equation (71) with $K_0 = 0$) so that the actual number of significant Bloch waves is $N_0(0)/2$.

The final step in the WKB approximation to the many-wave theory is to work out the values of the contributions of the stationary points $x_K^{\pm}(s)$ (equation (73)) to the integrals in equation (71). The stationary-phase formula (Erdelyi 1956, p. 51) involves the second derivative of the exponents in the integrands, that is (equations (67) and (69)) the function

$$\frac{\mathrm{d}^2\phi(0,x)}{\mathrm{d}x^2} = -\frac{u'(x)}{2\{s - u(x)\}^{1/2}}. \tag{85}$$

For the 'free' solutions (67) we only obtain contributions if K_G is positive (since we are taking K_0 as positive), and the sum of contributions from $x_K^+(s)$ and $x_K^-(s)$ is

$$\int_{-a/2}^{a/2} \mathrm{d}x\, \tau_j^+(x) \exp(-\mathrm{i}Kx) = \frac{2(2\pi)^{1/2} \cos\left[\phi\{0, x_K^+(s_j^+); s_j^+\} - Kx_K^+(s_j^+) + \pi/4\right]}{\left[|u'(x_K^+)| \int_{-a/2}^{0} \mathrm{d}x/\{s_j^+ - u(x)\}^{1/2}\right]^{1/2}}. \tag{86}$$

For the 'bound' solutions (69) we have

$$\int_{-a/2}^{a/2} \mathrm{d}x\, \tau_j(x) \exp(-\mathrm{i}Kx) = \frac{2\sqrt{\pi} \exp\{(\mathrm{i}/2)(K_0 a + j\pi)\} \cos\left[\pm\phi\{x_K^-(s_j), x_0^-(s_j); s_j\} + Kx_K^-(s_j) + \tfrac{1}{2}K_0 a + \tfrac{1}{2}j\pi\right]}{\left[|u'(x_K^+)| \int_{-a/2}^{x_0^-(s_j)} \mathrm{d}x/\{s_j - u(x)\}^{1/2}\right]^{1/2}} \tag{87}$$

where the upper and lower signs refer respectively to the cases where K is positive and negative.

If we insert the expressions (86) and (87) into equation (71) we obtain for $A_G(z)$, the amplitudes of the diffracted beams, the results

$$\left.\begin{aligned} A_G(z) = \frac{4\pi}{a} \sum_{s_j=l_1}^{0} \frac{\exp(-\mathrm{i}s_j z/2k) \cos B_{K_0}^+ \cos B_{K_G}^+}{CD_1} \\ + \frac{8\pi}{a} \sum_{s_j^+=0}^{l_2} \frac{\exp(-\mathrm{i}s_j^+ z/2k) \cos E_{K_0} \cos E_{K_G}}{CD_2} \end{aligned}\right\} (K < K_0^c;\, K_G < K_0^c;\, K_G > 0)$$

$$= \frac{4\pi}{a} \sum_{s_j = l_1}^{0} \frac{\exp(-\mathrm{i}s_j z/2k)\cos B_{K_0}^{+}\cos B_{K_G}^{-}}{CD_1} \qquad (K < K_0^c;\ |K_G| < K_0^c;\ K_G < 0)$$

$$= \frac{8\pi}{a} \sum_{s_j^{+} = l_1}^{l_2} \frac{\exp(-\mathrm{i}s_j^{+} z/2k)\cos E_{K_0}\cos E_{K_G}}{CD_2} \qquad (K_0 \text{ or } K_G > K_0^c) \tag{88}$$

where

$$l_1 = \max(K_G^2, K_0^2) - |u(-a/2)|$$

$$l_2 = \min(K_G^2, K_0^2)$$

$$B_K^{\pm} = \pm\phi\{x_K^{-}(s_j), x_0^{-}(s_j); s_j\} + Kx_K^{-}(s_j) + \tfrac{1}{2}K_0 a + \tfrac{1}{2}j\pi$$

$$E_K = \phi\{0, x_K^{+}(s_j^{+}); s_j\} - Kx_K^{+}(s_j) + \frac{\pi}{4}$$

$$C = \{u'(x_{K_0}^{+})\,u'(x_{K_G}^{+})\}^{1/2}$$

$$D_{1,2} = \int_{-a/2}^{x_0^{-}(s_j),\,0} \mathrm{d}x/\{s_j - u(x)\}^{1/2}$$

A particularly simple case of these formulae occurs for normal incidence, when K_0 is zero, for observation of the direct ($G = 0$) beam:

$$A_0(z) = \frac{4\pi}{a} \sum_{\substack{s_j<0 \\ j\,\text{even}}} \frac{\exp(-\mathrm{i}s_j z/2k)}{|u'(x_0^{+}(s_j))| \int_{-a/2}^{x_0^{-}(s_j)} \mathrm{d}x/\{s_j - u(x)\}^{1/2}} \tag{89}$$

The formulae (88) will be valid under semiclassical conditions; it would be difficult to specify these conditions precisely, since this would involve calculating correction terms to a series of expressions that are already very complicated. However, knowledge of the validity conditions of WKB formulae for simpler problems tells us that our results will be valid when there are many 'bound' states in the potential wells between the barriers at $x = na$, that is when there are many oscillations in a unit cell for the wave functions with s near zero; this occurs when $N_0(0)$ (equation (84)) greatly exceeds unity. If we had used the uniform parabolic cylinder function approximations for the eigenstates, which are valid for all x and s, instead of the exponential and Airy-function forms (61) and (62) which fail near $s = 0$, our final results (which would be expressible only as integrals over x, and not explicitly as in (89)) would give very good approximations whenever $N_0(0)$ exceeded unity—that is for all cases except the kinematic case. The edges of the band of contributing eigenvalues (figure 10) would not be sharp, so that the diffracted beams outside the range K_G^{-} to K_G^{+} would not have zero strength; instead, the fall-off in amplitude which occurs when the contributing regions of the integrals in equations (71) change from stationary points to end points would be described by the same Fresnel integrals as those governing the transition from light to shadow behind a sharp edge.

5. Transformation of amplitudes into classical form

When the number of contributing Bloch waves (equation (84)) is large, the eigenfunction

series (88) for the diffraction amplitudes $A_G(z)$ are difficult to evaluate and interpret. What we do to overcome this difficulty is to consider the j index, which specifies the eigenfunctions, as a continuous variable, and use the Poisson summation formula (Lighthill 1958) to transform the series; this formula is exact, and can be written as

$$\sum_{j=-\infty}^{\infty} f_j = \sum_{m=-\infty}^{\infty} \int_{-\infty}^{\infty} \mathrm{d}j f(j) \exp(\mathrm{i}jm2\pi) \tag{90}$$

where $f(j)$ is any smooth function of j which equals f_j when j is integral. It is much more convenient to integrate over s than over j, so we change variables, as follows:

$$\left.\begin{aligned} \Phi(s_j) = (j + \tfrac{1}{2})\pi; \quad \frac{4\pi}{a}\mathrm{d}j = \frac{4\pi}{a}\frac{\mathrm{d}j}{\mathrm{d}s}\mathrm{d}s = \frac{4}{a}\int_{-a/2}^{x_0^-(s)} \frac{\mathrm{d}x}{\{s-u(x)\}^{1/2}}\mathrm{d}s \\ (s<0) \\ \Phi(s_j^+) = +K_0 a + 2j^+\pi; \quad \frac{8\pi}{a}\mathrm{d}j^+ = \frac{8\pi}{a}\frac{\mathrm{d}j^+}{\mathrm{d}s}\mathrm{d}s = \frac{4}{a}\int_{-a/2}^{0} \frac{\mathrm{d}x}{\{s-u(x)\}^{1/2}}\mathrm{d}s \\ (s>0) \end{aligned}\right\} \tag{91}$$

where we have used equations (54), (56) and (65).

This transformation results in a series of oscillatory integrals for $A_G(z)$, which it is again natural to try to evaluate by the method of stationary phase. In order to bring out the essential points with the minimum of confusing detail, we shall select two special cases of equation (88) for closer study. The first case is where the inclination of the incident beam exceeds the critical angle θ_c; we are thus dealing with the last equation in equations (88), involving only 'free' Bloch states, which transforms according to equations (90) and (91) into

$$A_G(z) = \frac{4}{a}\sum_{m=-\infty}^{\infty} \int_{\max(K_0^2, K_G^2)-|u(-a/2)|}^{\min(K_0^2, K_G^2)} \mathrm{d}s \exp\left[\mathrm{i}\{sz/2k + 2m\phi(0, a/2; s) - mK_0 a\}\right] \times \frac{\cos\left[\phi\{0, x_{K_0}^+(s); s\} - K_0 x_{K_0}^+(s) + \pi/4\right] \cos\left[\phi\{0, x_{K_G}^+(s); s\} - K_G^+ x_{K_G}^+ + \pi/4\right]}{\left[u'\{x_{K_0}^+(s)\}\, u'\{x_{K_G}^+(s)\}\right]^{1/2}} \tag{92}$$

The two cosine functions consist of four exponentials which must be treated separately by the method of stationary phase. Use of the result

$$\frac{\mathrm{d}}{\mathrm{d}s}\left[\phi\{0, x_K^\pm(s); s\} - Kx_K^\pm(s)\right] = \frac{1}{2}\int_0^{x_K^\pm(s)} \frac{\mathrm{d}x}{\{s-u(x)\}^{1/2}} \qquad (K>0) \tag{93}$$

which is derived using equation (72) and which applies to all the similar phase functions in equations (88), leads to the following stationary-phase conditions for the s values contributing to the mth integral in equation (92):

$$\frac{z}{k} = \pm\int_0^{x_{K_0}^-(s)} \frac{\mathrm{d}x}{\{s-u(x)\}^{1/2}} \pm \int_0^{x_{K_0}^+(s)} \frac{\mathrm{d}x}{\{s-u(x)\}^{1/2}} + 2m\int_0^{a/2} \frac{\mathrm{d}x}{\{s-u(x)\}^{1/2}}. \tag{94}$$

The two $\pm$ signs are independent, and the fact that z is positive immediately tells us that those integrals where m is negative are negligible compared with the rest.

The solutions of equation (94) are

$$s \equiv s_i(K_0, K_G, z) \tag{95}$$

and we shall now show that these are precisely the s values for those classical paths which are incident on the slab at K_0 and which are travelling in the direction K_G at depth z.

From equation (81) we see that a given K_0 and point of entry $x(0)$ defines s for a ray. The later lateral positions $x(z)$ of this ray are related to its direction $K(z)$ by

$$\frac{K(z)}{k} = \frac{\mathrm{d}x(z)}{\mathrm{d}z} \tag{96}$$

an equation which is obvious but which can also be derived as one of Hamilton's equations after the 'time' variable is identified with $z/2k$ from (30). Combining equation (96) with equation (82) we obtain

$$\frac{\mathrm{d}x(z)}{\mathrm{d}z} = \{s - \bar{U}(x)\}^{1/2} \tag{97}$$

or

$$\frac{z}{k} = \int_{x(0)}^{x(z)} \frac{\mathrm{d}x}{\{s - \bar{U}(x)\}^{1/2}}. \tag{98}$$

This equation tells us the depth z reached by the ray that started out at $(x(0), K_0)$ and is now at $x(z)$ (which need not be in the same cell as $x(0)$); the direction of the ray is given by equation (82). Conversely, equation (98) also tells us what s—that is what entry point $x(0)$—is associated with these rays which start out in direction K_0 and have deviated to K at depth z.

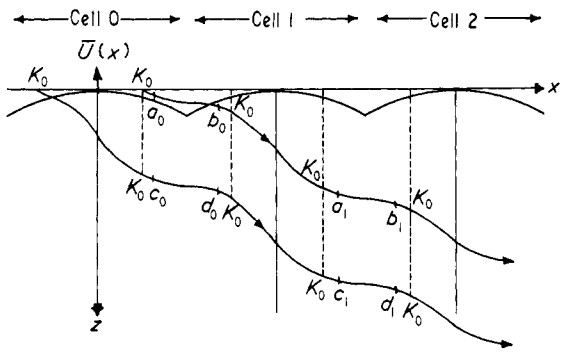

Figure 12. The four types of rays that have direction K.

To see how our equation (94) describes explicitly the totality of possible rays included in equation (98), we refer to figure (12) which shows the two rays that start out in a single cell with given values of K_0 and s. The points are shown where the rays regain their initial direction K_0 and where they have a direction K, chosen to exceed K_0 slightly. There are four types of ray, specified by a_m, b_m, c_m, d_m, the subscript m indicating that the ray has arrived at its final position after traversing m complete cells; these rays correspond to those specified by equation (94) according to the following scheme:

$$\left.\begin{aligned} a_m &\text{ corresponds to } && -, +, m \\ b_m &\text{ corresponds to } && -, -, (m+1) \\ c_m &\text{ corresponds to } && +, +, m \\ d_m &\text{ corresponds to } && +, -, (m+1) \end{aligned}\right\} \tag{99}$$

As an example, let us suppose that both signs are negative in equation (94), and that m equals two; then inspection of equation (99) shows that we are dealing with the ray labelled b_1 in figure 12.

Thus the Poisson summation formula automatically separates out the contributions from the topologically different contributing rays (cf. Berry 1969a). For a given z, K_0, K_G only a few of these possible rays actually contribute, since the quantity

$$2\int_0^{a/2}\frac{\mathrm{d}x}{\{s-u(x)\}^{1/2}}$$

is bounded as s varies among its permitted values.

Having established at last that these classical paths emerging from the slab in direction K_G contribute to the Gth diffracted beam, we must finally derive expressions for the value of the contributions. We shall only present the stationary-phase evaluations of the integrals in equation (92), bearing in mind that the presence of caustics and foci in the pattern of classical paths will cause these simple expressions to diverge, necessitating the use of uniform approximations involving more complicated functions (Berry 1969b). The phase of W_i, the contribution from the ith path, which is obtained by substituting s_i from equation (95) into the appropriate exponential in equation (92), is simply the classical action function along the ray going from $(x_{K_0}, 0)$ to (x_{K_G}, z) minus the phase $K_G x$ of the diffracted plane wave using the fact that the phase at $z = 0$ is $K_0 x(0)$, and that the extra contribution on traversing the slab is the 'time' (that is $z/2k$) integral of the 'Lagrangian' $K^2 - \bar{U}(x)$, we obtain

$$\begin{aligned}W_i(K_0,K_G,z) &= K_0x_0^i(K_0,K_G,z)+\frac{1}{2k}\int_0^z \mathrm{d}z'\,(K^2-\bar{U})-K_Gx_{K_G}^i(K_0,K_G,z)\\ &= K_0x_0^i+\frac{1}{2k}\int_0^z \mathrm{d}z'\,(2K^2-s_i)-K_Gx_{K_G}^i\\ &= -\frac{s_iz}{2k}+\int_{x_0^i}^{x_{K_G}^i}\mathrm{d}x\,\{s_i-\bar{U}(x)\}^{1/2}+K_0x_0^i-K_Gx_G^i \qquad (100)\end{aligned}$$

where the last form of writing comes from equations (96) and (97). The *amplitude* of the contribution of the ith path involves the square root of the second derivative of the phase in equation (92), evaluated at s_i. Thus the final semiclassical formula for the amplitudes is

$$A_G(z)=\frac{2\sqrt{\pi}}{a}\sum_i \alpha_i\frac{\exp\{iW_i(K_0,K_G,z)\}}{\left[u'(x_{K_0}^+(s_i))\,u'(x_{K_G}^+(s_i))\,\mathrm{d}/\mathrm{d}s_i\int_0^{x_{\bar{K}}(s_i)}\mathrm{d}x/\{s_i-u(x)\}^{1/2}\right]^{1/2}}. \qquad (101)$$

The amplitude factor is proportional to the density of paths in the contributing region, and it is this factor which diverges at a caustic or focus, while the phase factor α_i is an integral power of $\exp(\mathrm{i}\pi/4)$ which varies from ray to ray. The essential result to emerge from using the Poisson formula is that instead of the series (88) containing many contributions from the s_j of the Bloch waves we now have only a few contributions from the s_i of the classical paths.

Our second special case is chosen to involve only the 'bound' solutions where $s_j < 0$. This is the case of normal incidence where K_0 is zero, and we restrict ourselves to examining the forward beam when G is zero. Thus we apply the Poisson formula to equation (89), using the transformation (91) where the density of j states is halved because only the even eigenfunctions are involved. Thus we have the series of 'semiclassical' integrals

$$A_0(z)=\frac{2}{a}\sum_{m=-\infty}^{\infty}\int_{-|u(-a/2)|}^{0}\mathrm{d}x\,\frac{\exp\{-\mathrm{i}sz\,2k+\mathrm{i}m\,[2\phi\{-a/2,x_0^-(s),s\}-\pi,2]\}}{|u'(x_0^+(s))|} \qquad (102)$$

Since we are dealing with bound states, each s is associated with a turning point x by the relation (cf. equation (58))

$$s = u(x) \qquad (103)$$

so that the integrals transform easily into diffraction integrals over a half-cell:

$$A_0(z) = \frac{2}{a}\sum_{m=-\infty}^{\infty}\int_{-a/2}^{0} \mathrm{d}x \exp\left(-\mathrm{i}\frac{u(x)z}{2k} + \mathrm{i}m\left[2\int_{-a/2}^{x}\{u(x)-u(x')\}^{1/2}\,\mathrm{d}x' - \tfrac{1}{2}\pi\right]\right). \quad (104)$$

Once again we examine the points $x_m(z)$ where the exponents are stationary; simple differentiation yields the condition

$$\frac{z}{k} = 2m\int_{-a/2}^{x_m(z)} \frac{\mathrm{d}x'}{[u\{x_m(z)\}-u(x')]^{1/2}}. \quad (105)$$

Negative values of m are once again ruled out, and from the general classical formula (98) we see that once again it is the classical paths that contribute, the point $x_m(z)$ being the point of entry of a ray which starts out with $K = 0$ and traverses the bottom of the potential well, at $x = -a/2$, m times before emerging at depth z with K again equal to zero (figure 13). The pattern of paths, and hence the form of $A_0(z)$, differs greatly for positive and negative particles.

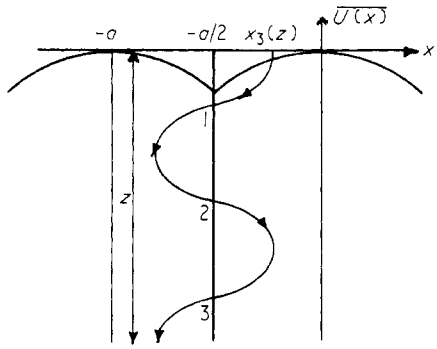

Figure 13. Typical ray contributing at normal incidence to forward beam.

For electrons the pattern of paths is as shown in figure 14(*a*) and equation (105) has solutions $x_m(z)$ for all positive m, whatever the depth z. As m increases, the contributing point moves in from $x = 0$ towards the centre of the potential well at $x = -a/2$. When we approximate equation (104) by the method of stationary phase, we must not approximate the $m = 0$ integral: if we do, then the resulting contribution will diverge at $z = 0$ since then all rays point along the forward direction. The resulting approximation is

$$A_0(z) = \frac{2}{a}\int_{-a/2}^{0} \mathrm{d}x \exp\left\{-\mathrm{i}z\frac{u(x)}{2k}\right\} + \frac{2}{a}\sum_{m=1}^{\infty} \left.\frac{(2\pi)^{1/2}\exp\{\mathrm{i}(\frac{1}{4}\pi - u\{x_m(z)\}z/2k + m[2\int_{-a/2}^{x_m(z)}\{u(x_m)-u(x')\}^{1/2}\,\mathrm{d}x' - \frac{1}{2}\pi])\}}{[mu'\{x_m(z)\}\,\mathrm{d}/\mathrm{d}x\int_{-a/2}^{0}\mathrm{d}x'/\{u(x)-u(x')\}^{1/2}]^{1/2}}\right|_{x=x_m(z)}, \quad (106)$$

The first integral is precisely the phase grating approximation considered in § 2 of this paper, and, as expected, it only dominates $A_0(z)$ for small z; for larger z, the entry points $x_m(z)$ of the contributing rays move out towards $x = 0$. The functions in equation (106) can be evaluated exactly for a quadratic potential

$$u(x) = -\alpha x^2 \quad (107)$$

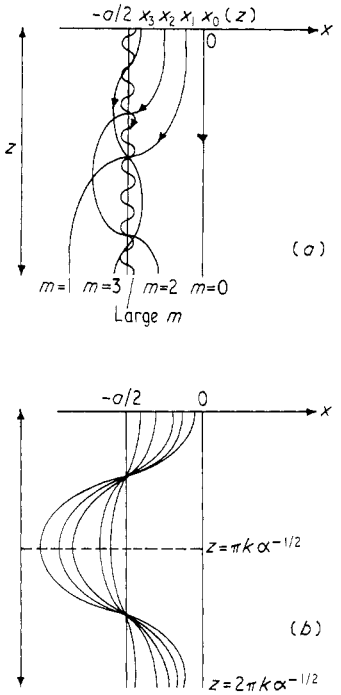

Figure 14. Patterns of paths contributing to forward beam at normal incidence for: (*a*) negative particles, (*b*) positive particles in a quadratic potential.

to give the result

$$A_0(z) = \frac{2}{a}\int_0^{a/2} \mathrm{d}x \exp\left(\mathrm{i}z\frac{\alpha x^2}{2k}\right) + \frac{2}{a}\sum_{m=1}^{\infty} \exp(\mathrm{i}\pi/4)\left\{\frac{\pi}{m\sqrt{\alpha}}\tanh\left(\frac{z\sqrt{\alpha}}{2km}\right)\right\}^{1/2} \times \exp\left[\mathrm{i}m\left\{\frac{a^2\sqrt{\alpha}}{4}\tanh\left(\frac{z\sqrt{\alpha}}{2km}\right) - \frac{\pi}{2}\right\}\right] \tag{108}$$

where the integral in the first term is a combination of sine and cosine Fresnel integrals. There are no caustics or foci in the pattern of figure 14(*a*), so that equation (108) does not diverge for any z.

In the case of positively-charged incident particles, equation (105) does not have solutions for all m for given z, basically because the integral in equation (105) (for $z = 1$) has a lower bound corresponding to particles near the smooth bottom of the potential well at $x = -a/2$. Thus caustics and foci can develop, the ray pattern becomes very complicated, and the stationary-phase method would frequently yield divergent results. This behaviour is most extreme for the quadratic potential analogous to equation (107), namely

$$u(x) = \alpha\left(|x| + \frac{a}{2}\right)^2 - \frac{\alpha a^2}{4}. \tag{109}$$

Then (figure 14(*b*)) there is perfect focusing, and there only exist forward-directed rays at the depths

$$z_m = \frac{m\pi k}{\sqrt{\alpha}} \tag{110}$$

when *all* the rays point in the forward direction. The stationary-phase method fails com-

pletely here, but the set of diffraction integrals (104) simply becomes a series of Fresnel integrals:

$$A_0(z) = \frac{2}{a} \sum_{m=-\infty}^{\infty} \int_0^{a/2} \mathrm{d}x \exp\left\{ \mathrm{i}x^2 \left(\frac{m\pi\sqrt{\alpha}}{2} - \frac{\alpha z}{2k} \right) - \frac{m\pi}{2} \right\}. \tag{111}$$

The mth integral in this expression is negligible under semiclassical conditions (large α) unless z is near to z_m, so that the amplitude $A_0(z)$, and the intensity $|A_0(z)|^2$ (figure 15) are sharply peaked about the points z_m. The fact that the classical pattern of paths is periodic in z means that the function $A_0(z)$ is periodic in the semiclassical approximation. The

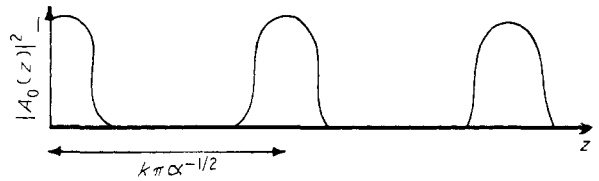

Figure 15. Intensity of forward beam when positive particles are incident normally on a quadratic potential.

WKB many-wave expressions (88) are also periodic, since when we approximate the 'bound' states by assuming that the barrier transmission coefficient $|T|$ is zero, the Bloch eigenvalues s_j are just the equally-spaced harmonic oscillator energy levels. However, the exact quantum $A_0(z)$ is not periodic, since when barrier penetration is taken into account the s_j are no longer equally spaced.

The simple asymptotic forms for the diffraction amplitudes, such as equation (101) or equation (108), can be written in the general form

$$A_G(z) = \sum_i a_i(K_G, z) \exp\{\mathrm{i}b_i(K_G, z)\} \tag{112}$$

where the index i distinguishes the different contributing classical paths, a_i represents the path density and b_i the action function. But the intensity corresponding to equation (112), namely

$$|A_G(z)|^2 = \sum_i \sum_j a_i a_j \exp\{\mathrm{i}(b_i - b_j)\} \tag{113}$$

cannot be the purely classical expression, because it involves the essentially wavelike feature of *interference* between the contributions. In the extreme classical limit, however, the phases b_i become very large (cf. equation (108) for large α), and the slightest departure of the incident beam from being perfectly monoenergetic or perfectly collimated will result in the different path contributions becoming incoherent with one another, so that one would in practice need the *average* value

$$|A_G(z)|^2_{\mathrm{av}} = \sum_i a_i^2(K_G, z). \tag{114}$$

Finally, in this limit the angular separation of the diffracted beams, λ/a, is so small that the separate $|A_G|^2$ cannot be resolved, and what is observed is a continuous fan of diffracted radiation (of width $2\theta_c$ for normal incidence) whose intensity in direction K at depth z is

$$I(K, z) = \sum_i a_i^2(K, z). \tag{115}$$

This is the purely classical quantity observed in proton channeling experiments.

6. Conclusions

In this paper a preliminary attempt has been made to clarify the subtle and complex

problem of the approach to the classical limit when waves traverse a periodic structure at high energies. To start with, § 2 consisted of a derivation of the high-energy approximation (equation (30)); in the course of the analysis, the PGA appeared as a zero-order approximation valid only for very thin crystals, and the concept of the parabolic cone of crystal contributing to the wave at its apex was useful in justifying the z-averaging of the potential function $U(\boldsymbol{r})$.

The rest of the paper consisted of an analysis of the high-energy approximation for the case of systematic reflections. In § 3 the exact many-wave solution of equation (30) was formulated in a way which stressed the spatial variation, rather than the Fourier coefficients of the potential.

Section 4 consisted of a WKB analysis of the many-wave theory, culminating in the expressions (88). The derivation showed that only a limited number (equation (83)) of Bloch waves, whose eigenvalues lie within a well-defined band, contribute to the amplitude of a given diffracted beam, and that the number of diffracted beams likely to appear (equation (77)) can be predicted on the basis of classical mechanics.

Finally, in § 5, it was shown that in fact of the band of contributing eigenvalues only those are important which correspond to those classical paths whose directions of incidence and emergence are the same as those of the incident and diffracted beams.

Work is in progress investigating how suitable the various formulae derived here are for numerical calculation.

Acknowledgments

The author would like to thank Dr J. W. Steeds for introducing him to this problem, and Mr A. C. Enfield for many helpful discussions.

References

BERRY, M. V., 1966, *Proc. Phys. Soc.*, **89**, 479–90.
—— 1967, *The Diffraction of Light by Ultrasound* (New York, London: Academic Press).
—— 1969 a, *J. Phys.* B: *Atom. molec. Phys.*, **2**, 381–92.
—— 1969 b, *Sci. Prog.*, **57**, 43–64.
CHADDERTON, L. T., 1968, *Phil. Mag.*, **18**, 1017–31.
COWLEY, J. M., 1968, *Phys. Lett.*, **A26**, 623–5.
COWLEY, J. M., and MOODIE, A. F., 1962, *J. Phys. Soc. Japan*, **17**, Suppl. B-II, 86–91.
DINGLE, R. B., 1956, *Appl. Sci. Res.*, **B5**, 345–67.
ERDELYI, A., 1956, *Asymptotic Expansions* (New York: Dover Publications).
FUJIWARA, K., 1961, *J. Phys. Soc. Japan*, **17**, 2226–38.
—— 1962, *J. Phys. Soc. Japan*, **17**, Suppl. B-II, 118–23.
GILL, S. P., 1964, *Harvard University Div. of Eng. and Appl. Phys. Tech. Mem.* No. 58.
HEADING, J., 1962, *An Introduction to Phase-Integral Methods* (London: Methuen).
HOWIE, A., 1966, *Phil. Mag.*, **14**, 223–37.
—— 1967, *Conf. on Solid St. Phys. with Accelerators* (Brookhaven National Labs Rep. No. BNL 50083 (C-52)).
HOWIE, A., and WHELAN, M. J., 1961, *Proc. R. Soc.*, **263**, 217–37.
LERVIG, P., LINDHARDT, J., and NIELSEN, V., 1967, *Nucl. Phys.*, **A96**, 481–504.
LIGHTHILL, M. J., 1958, *Introduction to Fourier Analysis and Generalised Functions* (London: Cambridge University Press), p. 67.
LINDHARDT, J., 1965, *Mat.-fys. Meddr. Dan. Vid. Selsk.*, **34**, No. 14.
MESSIAH, A., 1962, *Quantum Mechanis*, Vol. II (Amsterdam: North-Holland), p. 811.
MILLER, S. C., and GOOD, R. H., 1953, *Phys. Rev.*, **91**, 174–9.
RAMAN, C. V., and NATH, N. S. N., 1936, *Proc. Indian Acad. Sci.*, **3**, 459–65.
TAYLOR, J. G., 1970, *Quantum Mechanics: An Introduction* (London: Allen and Unwin) p. 97.